A Theory for Bjerknes Compensation: The Role of Climate Feedback

ZHENGYU LIU

Department of Atmospheric and Oceanic Sciences, and Nelson Center for Climate Research, University of Wisconsin–Madison, Madison, Wisconsin, and Laboratory for Climate and Ocean–Atmosphere Studies, Department of Atmospheric and Oceanic Sciences, School of Physics, Peking University, Beijing, China

HAIJUN YANG

Laboratory for Climate and Ocean–Atmosphere Studies, Department of Atmospheric and Oceanic Sciences, School of Physics, Peking University, Beijing, China

CHENGFEI HE

College of Atmospheric Sciences, Nanjing University of Information Science and Technology, Nanjing, China

YINGYING ZHAO

Laboratory for Climate and Ocean–Atmosphere Studies, Department of Atmospheric and Oceanic Sciences, School of Physics, Peking University, Beijing, China

(Manuscript received 25 March 2015, in final form 21 August 2015)

ABSTRACT

The response of the atmospheric energy (heat) transport (AHT) to a perturbation oceanic heat transport (OHT) is studied theoretically in a zonal mean energy balance model, with the focus on the effect of climate feedback, especially its spatial variation, on Bjerknes compensation (BJC). It is found that the BJC depends critically on climate feedback. For a stable climate, in which negative climate feedback is dominant, the AHT always compensates the OHT in the opposite direction. Furthermore, if local climate feedback is negative everywhere, the AHT will be weaker than the OHT (undercompensation) because of the damping on the surface oceanic heating through the top-of-atmosphere energy loss. One novel finding is that the compensation magnitude depends on the spatial scale of the forcing and is bounded between a minimum at the global scale and a maximum (of perfect compensation) at small scales. Most interestingly, the BJC is affected significantly by the spatial variation of the feedback, particularly a local positive climate feedback. As such, a regional positive feedback can lead to a compensating AHT greater than the perturbation OHT (overcompensation). This occurs because the positive feedback enhances the local temperature response, the anomalous temperature gradient, and, in turn, the AHT. Finally, the poleward latent heat transport leads to a temperature response with a polar amplification accompanied by a polar steepening of temperature gradient but does not change the BJC significantly. Potential applications of this BJC theory to more complex climate model studies are also discussed.

1. Introduction

The combined atmosphere–ocean system transports about 5 PW (1 PW = 10^{15} W) energy poleward (e.g., Trenberth and Caron 2001; Wunsch 2005). The partitioning of this total planetary energy (heat) transport (PHT) between the atmospheric energy (heat) transport (AHT) and oceanic heat transport (OHT) is important for constraining the response of the climate system. In a study of Atlantic climate variability, Bjerknes (1964) hypothesized that, in order to retain the year-to-year combined atmosphere–ocean heat transport, a change of OHT should be compensated by an opposite change in AHT, or the so-called Bjerknes compensation (BJC) hypothesis. Since the response of the top-of-atmosphere (TOA) energy flux depends on its feedback with temperature, it has long been recognized that the energy transport and then, potentially, the BJC could be related

Corresponding author address: Z. Liu, 1225 W. Dayton St., Madison, WI 53706.
E-mail: zliu3@wisc.edu

DOI: 10.1175/JCLI-D-15-0227.1

to climate feedback (e.g., Stone 1978a; Hwang and Frierson 2010; Zelinka and Hartmann 2012; Rose and Ferreira 2013; Feldl and Roe 2013a,b; Rose et al. 2014; Roe et al. 2015). In an earlier study of Earth's energy budget with an energy balance model (EBM), Stone (1978a) proposed that the PHT is determined essentially by the incoming shortwave radiation and the magnitude of the PHT is insensitive to the detailed structure and dynamics of the atmosphere–ocean system due to the efficient dynamic transport and negative feedback of thermal emission. Later studies confirm that the compensation of the AHT with OHT is valid to various extents in complex climate models. The compensation has been found valid in atmospheric general circulation models (AGCMs) coupled to a slab ocean for climate responses to various climate forcings (e.g., Manabe et al. 1975; Clement and Seager 1999; Kang et al. 2008, 2009; Herweijer et al. 2005; Frierson and Hwang 2012; Rose and Ferreira 2013; Donohoe et al. 2013; Seo et al. 2014); the compensation has also been found valid in coupled general circulation models (CGCMs) for decadal and longer-term internal climate variability (e.g., Shaffrey and Sutton 2006; van der Swaluw et al. 2007; Farneti and Vallis 2013) as well as climate responses to a perturbation OHT (e.g., Zhang and Delworth 2005; Cheng et al. 2007; Vellinga and Wu 2008; Broccoli et al. 2006; Vallis and Farneti 2009; Zhang et al. 2010; Yang et al. 2013; Farneti and Vallis 2013; Yang and Dai 2015).

In spite of these studies, important questions on BJC remain not fully understood, especially from the theoretical perspective. In simple model studies, the insensitivity of PHT to internal perturbation forcings, such as a perturbation OHT, implies a compensation between the AHT and OHT (e.g., Stone 1978a; Enderton and Marshall 2009; Kang et al. 2009; Hwang and Frierson 2010; Farneti and Vallis 2013; Seo et al. 2014). However, most previous studies have not focused on the mechanism that determines the magnitude of the BJC ratio (i.e., the ratio between the compensation AHT and the perturbation OHT). Indeed, modeling studies in complex climate models show a wide range of BJC ratios, from an AHT much smaller than the OHT (undercompensation) to comparable with the OHT (perfect compensation), and to even larger than the OHT (overcompensation); furthermore, the BJC ratio can vary significantly across latitudes (e.g., Vellinga and Wu 2008; Kang et al. 2008, 2009; Enderton and Marshall 2009; Vallis and Farneti 2009; Zhang et al. 2010; Farneti and Vallis 2013; Yang et al. 2013; Seo et al. 2014). These results lead to a question: what determines the magnitude of the BJC ratio, and why is the BJC ratio different in different regions?

Previous modeling studies imply that the BJC ratio could vary significantly with climate feedbacks, notably the cloud feedback and water vapor feedback in the tropics (e.g., Kang et al. 2008, 2009; Zhang et al. 2010; Zelinka and Hartmann 2012; Seo et al. 2014; Huang and Zhang 2014; Roe et al. 2015) and extratropics (e.g., Herweijer et al. 2005; Abbot and Tziperman 2008; Rose and Ferreira 2013) and the ice–albedo feedback in the polar region (e.g., North 1975; Enderton and Marshall 2009). The role of climate feedback in BJC in response to an OHT forcing has also been explored in some conceptual model studies, such as the two-box conceptual model of Rose and Ferreira (2013). However, the relation between climate feedback and BJC has not been studied systematically. In particular, almost all the simple model studies on the BJC to OHT forcing have assumed a spatially uniform negative feedback.[1] Yet, in complex climate models, and presumably the real world, climate feedback differs significantly in different regions not only in strength, but also in sign (e.g., Zhang et al. 1994; Taylor et al. 2011; Zelinka and Hartmann 2012; Rose et al. 2014; Feldl and Roe 2013a,b). This spatial variation of climate feedback has been suggested to be important in affecting global climate sensitivity in the context of global warming study (Armour et al. 2013; Roe et al. 2015).

This paper will focus on the role of the spatial variation of the feedback on the response of the energy transport to a perturbation OHT, in particular the BJC ratio, from the theoretical perspective. To shed light on the mechanism of BJC and its relation with climate feedback, especially its spatial variation, we will use a 1D EBM (North 1975; Frierson et al. 2007). To highlight the mechanism of the feedback on BJC, an idealized setting is used to allow for analytical solutions. Consistent with previous studies, such as that of Rose and Ferreira (2013) with a two-box model, in a stable climate system that is dominated by negative climate feedback our theory suggests that the BJC is valid, that is, the AHT is in the opposite direction to the perturbation OHT. The overall magnitude of the BJC ratio depends on the climate feedback relative to the efficiency of the AHT. More quantitatively, with negative climate feedbacks everywhere, the compensating AHT is always weaker than the perturbation OHT, leading to an undercompensation. One novel finding in our 1D EMB is that, with overall negative feedback, the BJC ratio depends on the spatial scale of the perturbation forcing, such that the BJC ratio is bounded between the

[1] Rose and Ferreira (2013) have studied the BJC in response to an OHT forcing in a two-box model, but with a uniform feedback. Roe et al. (2015) did use a 1D EBM with a spatially varying feedback but focused on the role of the nonuniform feedback on global mean climate sensitivity.

perfect compensation at the small-scale limit and an undercompensation at the planetary scale. Furthermore, as the negative feedback diminishes (or equivalently the efficiency of AHT increases), the AHT approaches the OHT, resulting in a perfect compensation. Most interestingly, when local climate feedback becomes positive, the compensating AHT can overwhelm the OHT, leading to an overcompensation. Finally, the inclusion of the spatial variation associated with the poleward latent heat transport tends to generate a polar amplification accompanied by a poleward steepening of the temperature gradient, but this latent heat transport does not change the BJC ratio significantly. The relevance of our theory to previous modeling studies will also be discussed.

The paper is arranged as follows. In section 2, we will study some basic constraints on the BJC under a spatially uniform climate feedback. Section 3 studies the BJC with a spatially varying climate feedback. Further issues related to the BJC theory are discussed in section 4, including the role of the latent heat transport and the application of our theory to understanding BJC studies in complex climate models. A summary is given in section 5.

2. BJC with uniform climate feedback

To better understand the mechanism of BJC, we use the zonally integrated EBM (Budyko 1969; Sellers 1969; North 1975). In an EBM, the TOA energy flux is parameterized as $A - BT$, where T is the surface temperature, A is the incoming shortwave radiation, and B is the net climate feedback parameter (Budyko 1969; Sellers 1969), which includes the net effect of temperature feedback, water vapor feedback, cloud feedback, and albedo feedback (Zhang et al. 1994; Soden et al. 2004; Soden and Held 2006; Zelinka and Hartmann 2012; Feldl and Roe 2013a,b). A stable global climate usually requires a negative global feedback, $-B < 0$.

In response to a perturbation surface energy flux F, the atmospheric energy is balanced by the convergence of AHT $-\partial_x \tilde{H}_A$ and the TOA energy flux $-BT$, as (North 1975)

$$-\partial_x \tilde{H}_A - B(x)T + F(x) = 0, \quad \text{for} \quad 0 < x < 1,$$

where x is the nondimensional meridional distance $x = \sin(\theta)$, with θ being the latitude. (For simplicity, we will here use the EMB on the plane instead of the sphere; see appendix A). The AHT will be parameterized as a Fickian diffusion of the moisture static energy (MSE) near the surface as $\tilde{H}_A = -\tilde{D}\partial_x \tilde{E}$, with $\tilde{D}$ being a constant transport coefficient (Frierson et al. 2007). The MSE consists of the sensible and latent heat as $\tilde{E} = (c_p + Lrq^*_{T_m})T$, where $c_p = 1000\,\mathrm{J\,kg^{-1}\,K^{-1}}$ is the specific heat, $r = 80\%$ is the relative humidity, $L = 2.5 \times 10^6\,\mathrm{J\,kg^{-1}}$ is the latent heat of vaporization, $q^*(T_m)$ is the saturation specific humidity as a function of the temperature of the mean state T_m, and $q^*_{T_m} = dq^*(T_m)/dT_m$. In the nondimensional form, the MSE budget for the atmosphere can be written as

$$\partial_{xx}[M(x)T] - b(x)T + f(x) = 0, \quad \text{for} \quad 0 < x < 1, \tag{2.1}$$

with the nondimensional AHT as

$$H_A = -\partial_x[M(x)T]. \tag{2.2a}$$

This moisture energy balance model (MEBM) depends critically on two nondimensional coefficients, the MSE coefficient $M(x)$ and the feedback parameter $b(x)$. The $M(x)$ is the MSE coefficient normalized by its global mean magnitude M_G as

$$M(x) = (1 + Lrq^*_{T_m}/c_p)/M_G,$$

where

$$M_G = \int_0^1 (1 + Lrq^*_{T_m}/c_p)\,dx, \tag{2.2b}$$

such that $\int_0^1 M(x)\,dx = 1$. The $M(x)$ values increases monotonically toward the equator because of the increasing T_m and, in turn, $q^*_{T_m}$. Since the surface temperature increases from ~−20°C at the pole to ~30°C at the equator in the real world, the latent heat coefficient $Lrq^*_{T_m}/c_p$ increases from ~0 to ~3. Therefore, M_G can be estimated approximately as a linear summation between the polar and equatorial region as $M_G \approx [(1 + 3) + (1 + 0)]/2 = 2.5$, and $M(x)$ ranges from ~0.4 in the polar region [=(1 + 0)/2.5)] to ~1.6 [=(1 + 3)/2.5] in the tropics, consistent with previous studies (e.g., Rose and Ferreira 2013; Roe et al. 2015). It is seen here that the latent heat transport has two effects: it increases the magnitude of the AHT transport coefficient $\tilde{D}$ to $\tilde{D}M_G$ and it leads to a spatial variation in $M(x)$. Hereafter, unless otherwise specified, we will focus on an equivalent "dry EBM" by setting $M(x) = 1$. This equivalent EBM includes the moisture effect on the magnitude of AHT transport coefficient, but neglects the effect of the spatial variation of the latent heat transport in $M(x)$. This is because, as will be seen in section 4 in the full MEMB (2.1), the latter effect can be discussed similarly as in the dry EBM after being absorbed into the variable feedback $b(x)$.

The feedback parameter $b(x)$ is the relative feedback parameter that represents the strength of the local

feedback relative to the MSE transport coefficient $D = \tilde{D}c_p M_G$ as

$$b = B/D. \tag{2.3}$$

Fitting the EBM to the present observation gives a $D = 0.6\,\mathrm{W\,m^{-2}\,K^{-1}}$ (North 1975), which is also consistent with recent EBM studies.[2] Although highly uncertain (e.g., Lindzen and Choi 2011; Feldl and Roe 2013b), B has been estimated from the present observations as $\sim 1.55\,\mathrm{W\,m^{-2}\,K^{-1}}$ (Sellers 1969; Kang et al. 2009; Rose and Ferreira 2013). Therefore, a reasonable value for the relative feedback is $b = 2.5$. In our discussion below, it should be kept in mind that b can be changed by both B and D. It should also be noted that, unlike in some EBM studies on the climatological mean state (North 1975), the feedback parameter here is prescribed constant with time and independent of climate dynamics. Thus, our EBM is best considered as the linear response to a small perturbation forcing f. where $f = F/D$ is the nondimensionalized climate forcing.

We will focus on the equilibrium climate response to a steady perturbation OHT H_O. The ocean surface heat flux is balanced by the OHT divergence as

$$f(x) = -\partial_x H_O, \quad \text{for} \quad 0 < x < 1. \tag{2.4}$$

We will study the single hemisphere solution here, such that the boundary fluxes vanishes at the "equator" $x = 0$ and the "pole" $x = 1$ in both H_A and H_O.

In this section, we first consider the simplest case of a uniform b. The climate response to heat flux forcing and, in turn, the BJC ratio, can be derived conveniently from the dry EMB (2.1) (with $M = 1$) in the eigenfunction of the diffusive operator: $\cos(n\pi x)$, $n = 1, 2 \ldots$. For $f(x) = f_n \cos(n\pi x)$, the corresponding OHT can be obtained from (2.4) as

$$H_O = -\frac{f_n}{n\pi}\sin(n\pi x). \tag{2.5}$$

The temperature response can be derived from the atmospheric energy budget (2.1) as

$$T(x) = T_n \cos(n\pi x), \quad \text{with} \quad T_n = \frac{f_n}{(n\pi)^2 + b}. \tag{2.6}$$

The corresponding AHT is therefore derived from Eq. (2.2) as

$$H_A = T_n n\pi \sin(n\pi x), \tag{2.7}$$

and the BJC ratio is therefore uniform with latitude as

$$C_n = \frac{H_A}{H_O} = \frac{-1}{1 + b/(n\pi)^2}, \quad n = 1, 2, \ldots. \tag{2.8}$$

It should be noted that this BJC ratio is independent of the parameterization of the ocean dynamics H_O and therefore is valid for a more general coupled ocean–atmosphere system as long as the atmosphere energy budget can be approximated as in the EBM (2.1) as (2.2).

Equation (2.8) shows that the AHT always compensates the OHT ($C < 0$) as long as climate feedback is nonpositive $-b \le 0$, which corresponds to a stable climate with respect to a climate perturbation. The stability can be seen easily by substituting $T(t, x) = e^{\lambda t}T(x)$ into the full slab ocean budget equation that includes the heat storage in (2.4) as

$$f(x) = -\partial_x H_O - \partial_t T, \tag{2.9}$$

as well as the atmospheric Eq. (2.1) (with $M = 1$). The eigenvalue is simply

$$\lambda = b, \tag{2.10}$$

and $b \ge 0$ ensures a stable climate. Note that, unlike the BJC ratio (2.8) that is independent of ocean dynamics, the temporal variability in Eq. (2.9), and in turn the eigenvalue (2.10), is valid only for a slab ocean. Active ocean dynamics can introduce additional unstable modes, such as the thermohaline mode associated with salinity advection feedback (e.g., Stommel 1961; Marotzke and Stone 1995; Rahmstorf 1996). Nevertheless, for the global mean mode, the transport term vanishes and (2.10) is still the eigenvalue. Therefore, $b \ge 0$ provides a necessary condition for climate stability regardless of the parameterization of ocean dynamics.

It is interesting from Eq. (2.8) that $|C|$ depends on the spatial scale, and it increases from the lower bound at the planetary scale to the upper bound at the small scale as

$$\frac{1}{1 + b/\pi^2} = |C_1| \le |C_n| < |C_\infty| = 1. \tag{2.11}$$

The first mode C_1 corresponds to the BJC derived from a two-box model of Rose and Ferreira (2013). Here, our 1D model also shows explicitly all the higher modes.

[2] For example, the corresponding coefficient for the sensible heat $\tilde{D}c_p$ can be calculated as ~0.25 and $0.22\,\mathrm{W\,m^{-2}\,K^{-1}}$ in Kang et al. (2009) and Rose et al. (2014), respectively. These values will give a D of $\sim 0.6\,\mathrm{W\,m^{-2}\,K^{-1}}$ using the MSE coefficient magnitude of $M_G \approx 2.5$.

With zero feedback $b = 0$, $|C| = 1$ is the perfect compensation, and the energy budget (2.1), (2.2), and (2.4) are reduced to a perfect balance between the convergence of AHT and OHT:

$$-\partial_x(H_A + H_O) \equiv \partial_{xx}(MT) + f(x) = 0, \quad 0 \le x \le 1. \tag{2.12a}$$

As such, the PHT is spatially uniform:

$$H_A + H_O = \text{const}, \quad 0 \le x \le 1. \tag{2.12b}$$

In addition, the PHT vanishes at both the pole and equator due to the no-flux boundary condition:

$$H_A = H_O = 0, \quad \text{at} \quad x = 0, \quad \text{and} \quad 1. \tag{2.13}$$

With a negative feedback $-b < 0$, BJC always exhibits an "undercompensation" $|C| < 1$. Now, the anomalous surface heating in direct response to the OHT is "damped" into the space through TOA, leaving less energy to transport back in the atmosphere. Equation (2.1) shows that $|C|$ is determined by the spatial scale n and the relative feedback b. The value of $|C|$ increases to the perfect compensation at the small-scale limit $n \to \infty$ because the AHT convergence increases with the "wavenumber" as $\partial_{xx} \sim n^2$, and therefore can overwhelm the local feedback, rendering (2.1) to a perfect compensation (2.12). This implies that a smaller-scale forcing has a greater efficiency in its dynamic transport and, in turn, a more perfect compensation. This scale dependence of BJC may help understanding the absence of fine structure in the latitudinal profile of the observed PHT (Stone 1978a) and its insensitivity to the details of the perturbation climate forcings (Enderton and Marshall 2009). That is, a small-scale change in OHT is compensated by the AHT completely, leaving little change in PHT.

Given a negative feedback, the minimum compensation is achieved at the planetary scale as $|C_1|$. This compensation ratio decreases with b, which, according to (2.3), can be caused either by a stronger negative feedback B, or, consistent with previous studies, by a less efficient dynamic transport D (Stone 1978a; Kang et al. 2009; Farneti and Vallis 2013; Rose and Ferreira 2013). In this case of uniform feedback, within the realistic range of the feedback parameter, however, this dependence on relative feedback is not very strong. Indeed, $|C_1|$ decreases from 1 to 0.5 when b increases from 0 to 10 (Fig. 1). With a typical feedback $b = 2.5$, $|C_1| \approx 0.8$. Figure 2 shows an example of the climate response to a smooth heat flux forcing $f = P_2(x) = (3x^2 - 1)/2$ (see appendix A), with $b = 2.5$.

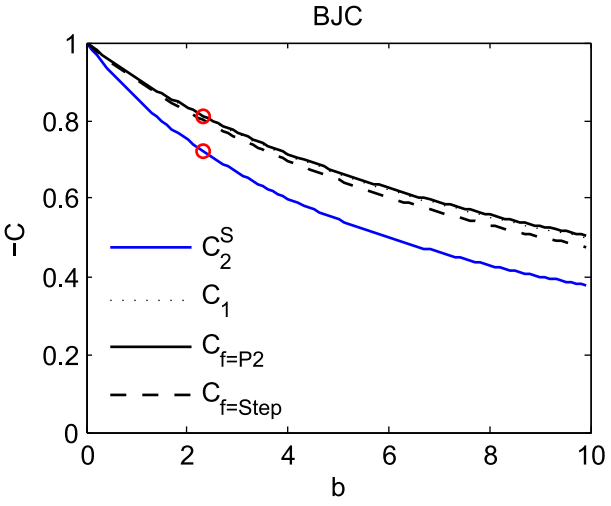

FIG. 1. Global mean BJC ratio as a function of the strength of the uniform negative feedback b for the sphere solution (C_2^S, blue) and plane solution ($C_{f=P2}$, black solid) forced by the Legendre polynomial $P_2(x)$, plane solution forced by $\cos(\pi x)$ (C_1, black dotted) and by the step function (3.2) (or Fig. 3d) ($C_{f=\text{Step}}$, black dashed). Note that C_2^S and C_1 are zonally uniform because the forcings are the eigenfunctions of the respective transport operator; C_1 is visually indistinguishable from $C_{f=P2}$. The two red circles represent the solution of $b = 2.5$ forced by $P_2(x)$ on the sphere and plane as shown in Fig. 2.

The poleward OHT (Fig. 2b, black) leads to a bipolar seesaw response of polar warming/tropical cooling (Fig. 2a). This temperature response induces a TOA radiation that damps the surface heating effect (Fig. 2d), leaving only ~80% of the energy to be transported equatorward in the atmosphere (Fig. 2c). The BJC ratio is not a constant because the forcing $P_2(x)$ is not an eigenfunction of the Cartesian diffusive operator ∂_{xx} here. Nevertheless, the BJC ratio is rather uniform and tracks closely with $C_1 \approx -0.8$, because this forcing projects dominantly on the first eigenmode $\cos(1\pi x)$.

It should be pointed out that all the conclusions of the plane solution here hold in the sphere solution after replacing the eigenfunction to the Legendre polynomials $P_m(x)$ (see appendix A) (Fig. 2, blue). In particular, the magnitude of the BJC ratio is smaller only slightly in the plane solution than in the spherical solution, by ~10%–20%, for a wide range of b values. (Fig. 1). Although very crude, it is interesting to note that a BJC ratio of around 70% seems to be largely consistent with the maximum BJC ratio in the extratropics in many previous CGCM studies (e.g., Zhang and Delworth 2005; van der Swaluw et al. 2007; Vellinga and Wu 2008; Zhang et al. 2010; Yang et al. 2013).

The physical mechanism for the undercompensation is simple. For, say, a poleward perturbation OHT, the

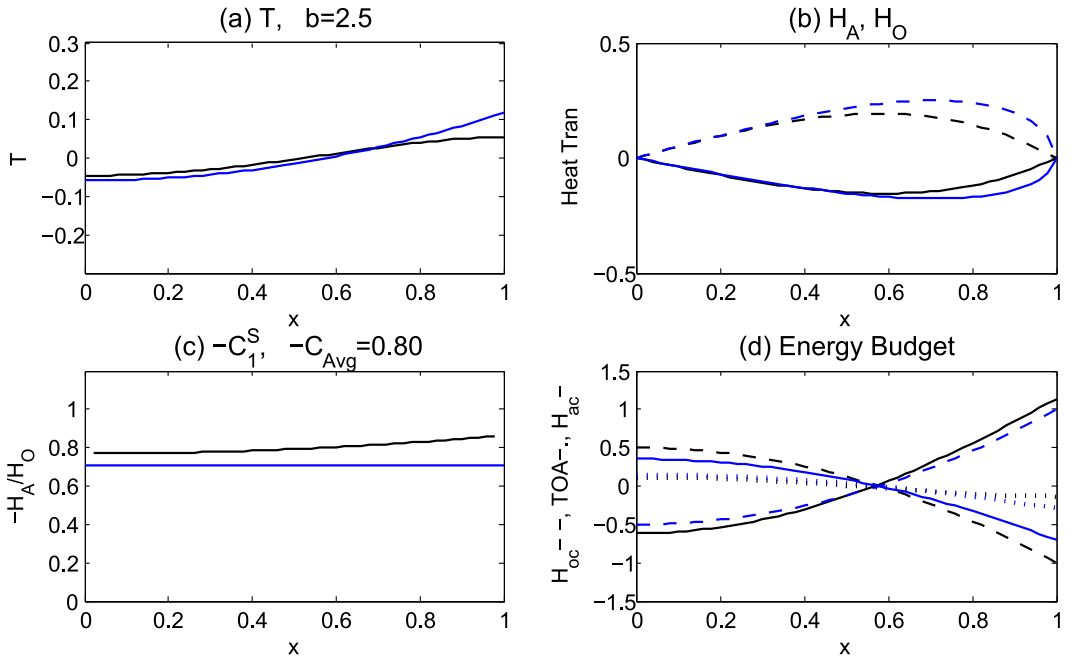

FIG. 2. Climate responses to the forcing $f(x) = P_2(x)$ for the sphere (blue) and plane (black) solution with a uniform negative feedback $b = 2.5$. (a) Temperature, (b) atmospheric (solid) and oceanic (dashed) heat transports, (c) BJC ratio, and (d) energy budget, showing $f(x)$ (dashed; same for the plane and sphere solutions), convergence of atmospheric heat transport (solid), and TOA radiative flux (dotted).

heat transport from the tropics to the extratropics in the ocean tends to induce extratropical warming and tropical cooling. This extratropical warming/tropical cooling will then generate an AHT toward the tropics, compensating the OHT. With a negative feedback everywhere, the anomalous temperature is damped everywhere through the TOA radiation. As such, the extratropical warming/tropical cooling is weaker and this leaves less energy to be transported back in the atmosphere, corresponding to an undercompensation. It is conceivable that if the local feedback turns positive in certain region, the anomalous temperature may no longer be damped there and the undercompensation may no longer hold. For example, a positive feedback in the tropics will amplify the tropical cooling induced by the OHT and therefore increase the anomalous temperature gradient with the extratropics (warming). The increased temperature gradient will then force a stronger equatorward AHT than the original OHT forcing, leading to an overcompensation. This overcompensation will be demonstrated next in the study of BJC with a nonuniform feedback.

3. BJC with nonuniform climate feedback

We now study BJC with nonuniform climate feedback $b(x)$. This is partly motivated by the BJC studies in many complex climate models that exhibit overcompensation locally in some regions (e.g., Vellinga and Wu 2008; Kang et al. 2008, 2009; Zhang et al. 2010; Yang et al. 2013; Seo et al. 2014). Yet, the uniform feedback solution (2.8) shows undercompensation everywhere for a stable climate. Indeed, all previous EBM studies on BJC response to OHT forcing have adopted a uniform feedback, and all of them have shown undercompensation (e.g., Stone 1978a; Enderton and Marshall 2009; Kang et al. 2009; Hwang and Frierson 2010; Farneti and Vallis 2013; Seo et al. 2014) except for one. Rose and Ferreira (2013) generate an overcompensation in their two-box model with a uniform negative feedback. This overcompensation is generated, however, by representing the effect of the positive cloud feedback in the extratropics as a reduction of the local heat flux forcing, instead of a positive local feedback. It will be seen below that, this overcompensation can indeed be reproduced in our model naturally with a local positive feedback.

To interpret the overcompensation in complex climate models, we hypothesize that a regional positive feedback, while maintaining a stable climate, can generate overcompensation as inferred from (2.8). Indeed, many recent modeling studies suggest dramatic spatial variation in local feedback. Many studies show a net positive feedback in the tropics due to the strong positive water vapor

feedback and cloud feedback (e.g., Taylor et al. 2011; Zelinka and Hartmann 2012; Feldl and Roe 2013a,b). This spatial variation of feedback has been recognized to affect the global mean climate sensitivity (Armour et al. 2013; Rose et al. 2014; Roe et al. 2015); but, its role on BJC has not been studied.

For our interest in planetary-scale responses, we will adopt an idealized two-zone setting, such that the feedback and forcing are both assumed uniform in the "tropics" $0 < x < X$ (zone 1) and "extratropics" $X < x < 1$ (zone 2) as

$$b(x) = \begin{cases} b_1 & 0 < x < X \\ b_2 & X < x < 1 \end{cases}, \tag{3.1}$$

$$f(x) = \begin{cases} f_1 & 0 < x < X \\ f_2 & X < x < 1 \end{cases}. \tag{3.2}$$

With the boundary conditions $H_A = 0$, at $x = 0$ and 1, and the matching conditions of continuous temperature and heat flux across the interzone boundary

$$T\,|\,(x \to X^-) = T\,|\,(x \to X^+),$$
$$M\partial_x T\,|\,(x \to X^-) = M\partial_x T\,|\,(x \to X^+),$$

the temperature response can be derived from (2.1) (with $M = 1$) as

$$T(x) = \begin{cases} \dfrac{G}{\sqrt{b_1}} \dfrac{\cosh(\sqrt{b_1}x)}{\sinh(\sqrt{b_1}X)} + T_{f1}, & 0 \le x \le X, \\ \dfrac{G}{\sqrt{b_2}} \dfrac{\cosh[\sqrt{b_2}(x-1)]}{\sinh[\sqrt{b_2}(X-1)]} + T_{f2}, & X \le x \le 1, \end{cases} \tag{3.3}$$

where

$$T_{fi} = \frac{f_i}{b_i}, \quad i = 1, 2 \tag{3.4}$$

are the local radiative equilibrium responses, and the coefficient G is

$$G = \frac{T_{f2} - T_{f1}}{\dfrac{\coth(\sqrt{b_1}X)}{\sqrt{b_1}} + \dfrac{\coth[\sqrt{b_2}(1-X)]}{\sqrt{b_2}}}. \tag{3.5}$$

The corresponding AHT is

$$H_A(x) = \begin{cases} H_{AX} \dfrac{\sinh(\sqrt{b_1}x)}{\sinh(\sqrt{b_1}X)}, & 0 \le x \le X, \\ H_{AX} \dfrac{\sinh[\sqrt{b_2}(x-1)]}{\sinh[\sqrt{b_2}(X-1)]}, & X < x \le 1, \end{cases} \tag{3.6}$$

with $H_{AX} \equiv H_A(X) = -G$. Since the global mean surface flux is assumed zero $\int_0^1 f(x)\,dx = 0$, the OHT can be written as

$$H_O(x) = \begin{cases} H_{OX}(x/X), & 0 \le x < X \\ H_{OX}(x-1)/(X-1), & X < x \le 1 \end{cases}, \tag{3.7}$$

where

$$H_{OX} \equiv H_O(X) = -Xf_1 = (1-X)f_2.$$

The BJC ratio can therefore be derived as

$$C(x) = \frac{H_A(x)}{H_O(x)} = \begin{cases} C_X \dfrac{\sinh(\sqrt{b_1}x)}{\sinh(\sqrt{b_1}X)} \dfrac{X}{x}, & 0 \le x \le X, \\ C_X \dfrac{\sinh[\sqrt{b_2}(x-1)]}{\sinh[\sqrt{b_2}(X-1)]} \dfrac{X-1}{x-1}, & X < x \le 1, \end{cases} \tag{3.8a}$$

with

$$C_X \equiv C(X) = \frac{H_{AX}}{H_{OX}} = \frac{-\left[\dfrac{1}{b_1 X} + \dfrac{1}{b_2(1-X)}\right]}{\dfrac{\coth(\sqrt{b_1}X)}{\sqrt{b_1}} + \dfrac{\coth[\sqrt{b_2}(1-X)]}{\sqrt{b_2}}}. \tag{3.8b}$$

For negative feedbacks everywhere, $-b_1, -b_2 < 0$, Eq. (3.8) shows an undercompensation everywhere $-1 < C_X \le C(x) < 0$, consistent with the uniform feedback solution (2.8). The maximum compensation occurs at $x = X$, because of the abrupt change and, in turn, small-scale forcing there, which tends to "drag" the BJC toward the perfect compensation, as discussed in (2.8). Figure 3 (black) shows an example of uniform negative feedback $b_1 = b_2 = 2.5$ and $X = 0.5$. Compared with the response forced by a smooth forcing $P_2(x)$ (Fig. 2, plane solution in black), the latitudinal structure of the surface forcing and in turn the energy budget show significant differences

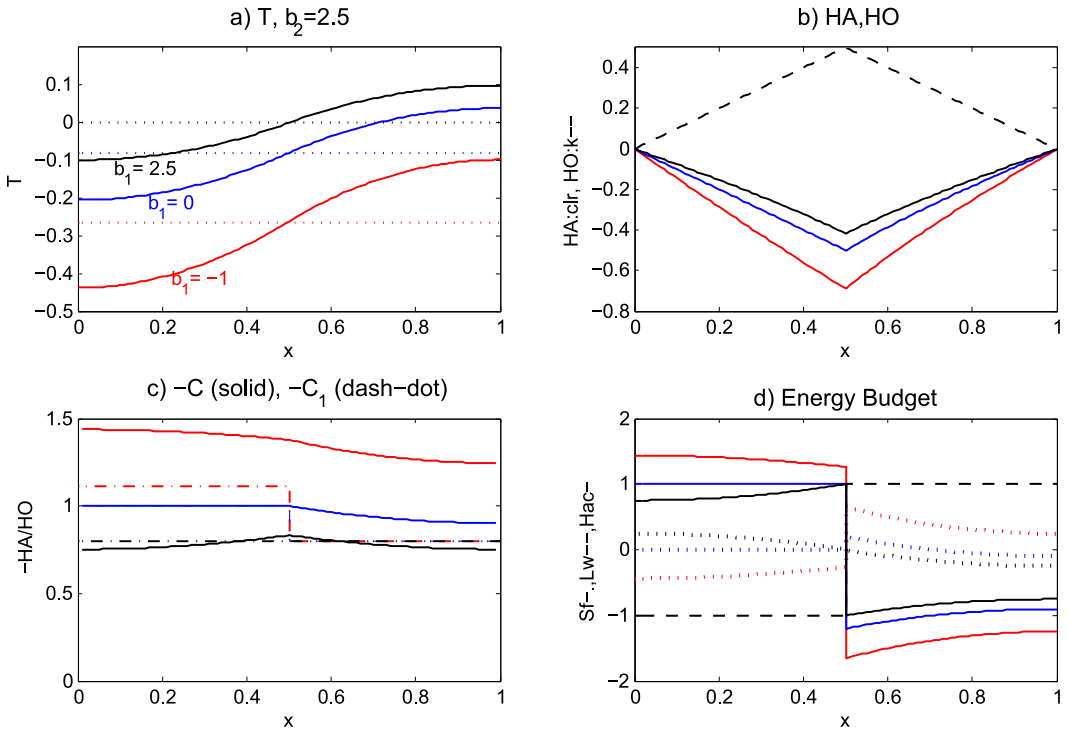

FIG. 3. Climate response similar to Fig. 2, but for the two-zone plane solution (with $X = 0.5$) in response to the step function forcing $f(x)$ [dashed line in in (d)]. The extratropical feedback is fixed at $-b_2 = -2.5$ while the tropical feedback $-b_2$ changes from -2.5 (black) to 0 (blue) and eventually to 1 (red). (a) Temperature (solid) with global mean temperature (dashed), (b) atmospheric (solid) and oceanic (dashed) heat transports, (c) BJC ratio C (solid) and the local estimation $C_1(x)$ (dash-dotted), and (d) the energy budget, $f(x)$ (dashed, same for all cases), convergence of the atmospheric heat transport (solid), and TOA radiative flux (dotted).

(Fig. 3d vs Fig. 2d), leading to different heat transports (Fig. 3b vs Fig. 2b). Nevertheless, both BJC structures remain rather uniform around $C_1 \sim -0.8$ (black in Fig. 2c vs Fig. 3c). This occurs because both $P_2(x)$ and the step function forcing (3.2) are dominated by the planetary-scale component, which forces the mode 1 BJC ratio C_1.

As the tropical negative feedback diminishes ($b_1 \to 0$), one can show from (3.8) that $C(x) \to -1$, and therefore the entire tropics approaches the perfect compensation. As discussed for Eqs. (2.12) and (2.13), the zero feedback here, combined with the no-flux boundary conditions, $H_A = H_O = 0$, at $x = 0$, leads to the perfect compensation. This perfect compensation in the tropics can be seen in the case of $b_1 = 0$ and $b_2 = 2.5$ (Fig. 3c, blue). Furthermore, it is interesting that the zero feedback in the tropics has a remote impact on the extratropics such that $|C|$ is enhanced toward the perfect compensation (Fig. 3c), even through local feedback there remains unchanged at $b_2 = 2.5$. This remote "spillover" effect of local positive feedback is caused by the heat transport.

Most interesting is the case where the tropical feedback becomes positive. A positive feedback in the tropics, coexisting with a negative feedback in the extratropics, is consistent with positive climate feedbacks in the tropics associated with water vapor feedback and cloud feedback (Philander et al. 1996; Gregory and Mitchell 1997; Clement and Seager 1999; Winton 2003; Clement et al. 2009; Hwang and Frierson 2010; Zelinka and Hartmann 2012; Feldl and Roe 2013a). In our EBM coupled with a slab ocean, the coupled system remains stable with a local positive feedback as long as the global mean feedback $-\overline{b} = -[b_1 X + b_2(1 - X)]$ remains slightly negative (appendix B; see Fig. 4b). Yet, a positive feedback in the tropics immediately leads to overcompensation,[3] as

[3] If $b(x) = 0$ is prescribed in a region away from either $x = 0$ or 1, there is no guarantee of a perfect local compensation $C = -1$. Now, the constant PHT depends on the C in its zone boundaries. Thus, overcompensation may not occur exactly when the local $-b(x) > 0$. Nevertheless, our numerical experiments show that $|C|$ tends always to be enhanced, and can achieve overcompensation if the local positive feedback is sufficiently strong (yet still maintaining climate stability).

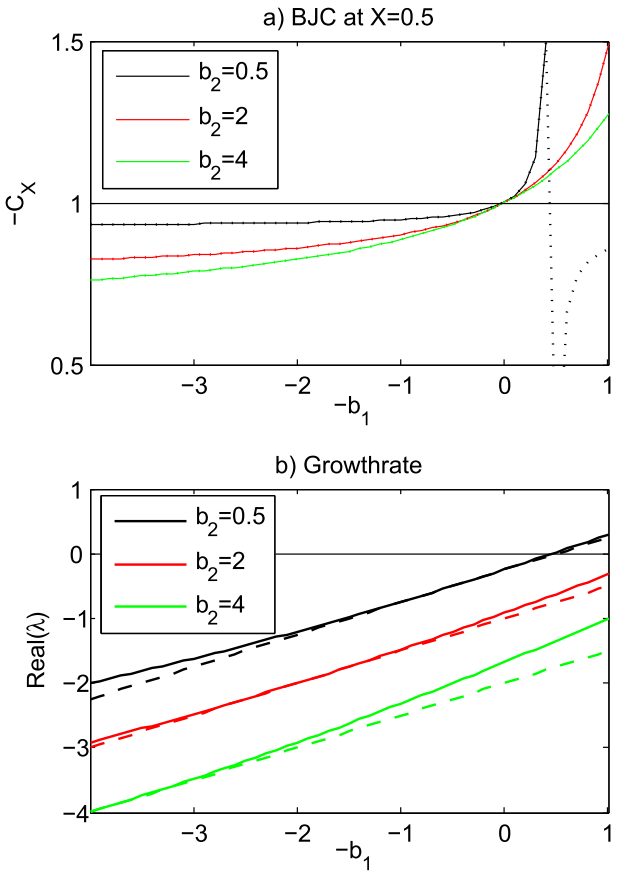

FIG. 4. (a) BJC ratio at the interzone boundary $X = 0.5$ as a function of the tropical feedback $-b_1$ for three extratropical feedbacks $b_2 = 0.5$, 2, and 4. Solid lines indicate stable solutions as judged from the eigenvalue in (b). The BJC ratio is not very sensitive to b_1 when $-b_1$ is negative, but increases rapidly with $-b_1$ when it becomes positive. (b) Growth rate of the least damped mode for each solution in (a) (solid). The growth rates are calculated form the eigenvalue Eq. (B3) (see appendix B). Also shown are the global mean feedback $-b_m = -[Xb_1 + (1 - X)b_2]$ (dashed). The growth rate approaches the global mean feedback when b_1 approaches b_2 (uniform feedback) and, in general cases, is slightly more positive than $-b_m$ when b_1 deviates away from b_2.

shown analytically below. Substituting $\sqrt{b_1} = i\sqrt{|b_1|}$, the tropical response in (3.8) becomes

$$C(x) = C_X \frac{\sin(\sqrt{|b_1|}x)}{\sin(\sqrt{|b_1|}X)} \frac{X}{x}, \quad \text{for} \quad 0 \le x \le X, \tag{3.9a}$$

where

$$C_X = \frac{\left[\dfrac{1}{|b_1|X} - \dfrac{1}{b_2(1-X)}\right]}{\dfrac{\cot(\sqrt{|b_1|}X)}{\sqrt{|b_1|}} - \dfrac{\coth[\sqrt{b_2}(1-X)]}{\sqrt{b_2}}}. \tag{3.9b}$$

As $b_1 \to 0$, we have the BJC ratio at X as

$$C_X \to -\left(1 + \frac{|b_1|X}{b_2(1-X)}\{\sqrt{b_2}(1-X) \times \coth[\sqrt{b_2}(1-X)] - 1\}\right).$$

Since $y \coth y \ge 1$ always holds, we have $|C_X| \ge 1$. Figure 4a shows C_X as a function of tropical feedback $-b_1$ for three negative extratropical feedback $-b_2$. When the tropical feedback is negative, $|C_X|$ is undercompensation and the ratio is not very sensitive to b_1. However, after the tropical feedback becomes positive, $|C_X|$ becomes overcompensation and the magnitude increases rapidly with the feedback strength until the solution is destabilized.

The structure of the climate response in the case of a modestly positive tropical feedback $-b_1 = 1$ is shown in Fig. 3 (red). Now, the overcompensation extends into the extratropics in spite of negative feedback there (Fig. 3c, red). The maximum $|C| \sim 1.4$ now occurs at the equator and decreases poleward to $X = ½$, and then toward the pole. This poleward decrease of overcompensation can be confirmed from the solution. For a modestly positive feedback $\sqrt{|b_1|}X < \pi/2$, $|C|$ decreases monotonically in the tropics from the equator toward X as in (3.9a), and then in the extratropics toward the pole as in (3.8a). Therefore, a positive tropical feedback leads to an overcompensation in the tropics, which then "spills over" into the extratropics (e.g., Fig. 3c, red).

The spillover of overcompensation into the extratropics suggests that local positive feedback plays the dominant role in determining the BJC ratio not only locally in the tropics, but also remotely in the extratropics. This point can be seen more clearly in another set of solutions (Fig. 5) where the tropical feedback $-b_1$ also increases from -2.5 to 1 as in Fig. 3, but the global mean feedback $-\bar{b}$ remains negative at -2.5, with a more positive $-b_1$ accompanied by a more negative $-b_2$ (Fig. 5d). In spite of the strengthened negative feedback in the extratropics, the response now remains similar to those in Fig. 3. In particular, in the tropics, C approaches the perfect compensation when $b_1 = 0$ and is then enhanced to overcompensation when $-b_1 = 1$; furthermore, in the extratropics, $|C|$ increases, although the local feedback becomes even more negative.

The effect of local positive feedback can also be seen in comparison with a local estimation of the BJC ratio for mode 1 in Eq. (2.8):

$$C_1(x) = -1 \Big/ \left[1 + \frac{b(x)}{\pi^2}\right] \tag{3.10}$$

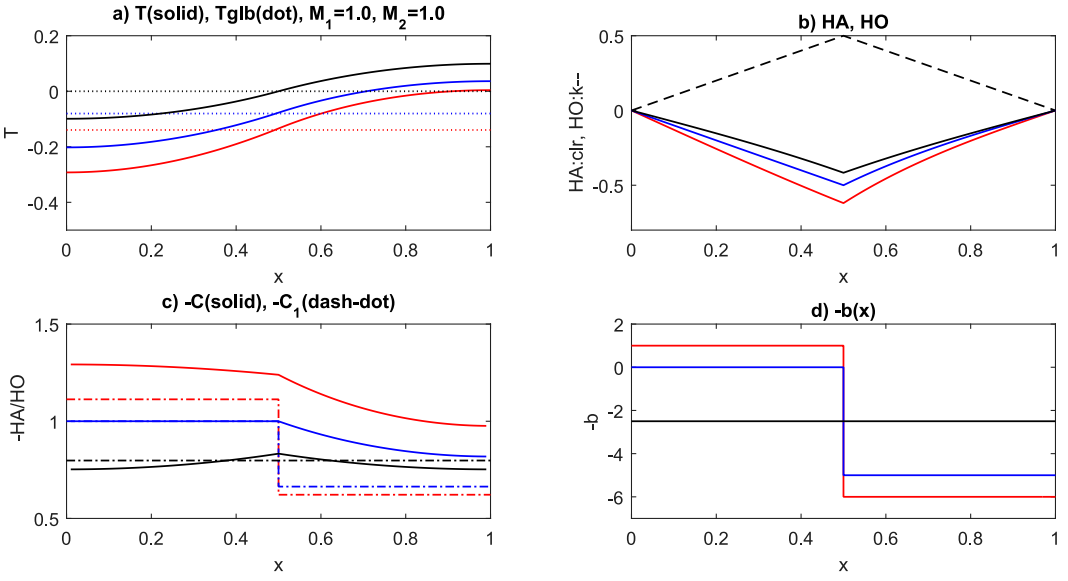

FIG. 5. Climate response of the two-zone solution (with $X = 0.5$) similar to Fig. 3, but now with a fixed negative global mean feedback -2.5. The tropical feedback changes from negative feedback $-b_1 = -2.5$ (black) to 0 (blue) and eventually a positive feedback 1 (red), while the extratropical feedback $-b_2$ becomes more negative, as shown in (d) for the profile of $b(x)$, such that the global mean $[Xb_1 + (1 - X)b_2] = 2.5$. (a) Temperature (solid) with the global mean temperature (dashed), (b) atmospheric (solid) and oceanic (dashed) heat transports, and (c) BJC ratio C (solid) and the local estimation C_1 (dash-dotted).

(dash-dotted in Figs. 3c and 5c). This estimation can be regarded as a Wentzel–Kramers–Brillouin (WKB) approximation (Bender and Orszag 1978) of the local $C(x)$ for a slowly varying negative feedback $b(x)$. The comparison with the true $C(x)$, however, shows that this local estimation $C_1(x)$ severely underestimates $|C(x)|$ when the feedback changes significantly in space. In particular, in the remote extratropics, when the tropical feedback becomes positive, the true $C(x)$ exhibits overcompensation, while the local estimation $C_1(x)$ remains low in undercompensation (red in Figs. 3c and 5c), rendering the local estimation (3.10) invalid.

Physically, the change of BJC ratio with feedback can be understood as follows. The poleward OHT (Figs. 3b and 5b) tends to generate an extratropical warming/tropical cooling. The poleward temperature gradient then generates an AHT equatorward, compensating the OHT. With a negative feedback, the extratropical warming/tropical cooling is damped through the TOA radiation, reducing the imbalance of local radiative equilibrium and leaving less energy to transport back by the AHT (Fig. 3d, black). As the negative feedback in the tropics becomes positive, the cooling in the tropics is amplified. This leads to an increase in the temperature gradient (blue and red, Figs. 3a and 5a), the AHT (blue and red, Figs. 3b and 5b) and eventually the overcompensation (Figs. 3c and 5c). Furthermore, the enhanced temperature gradient in the tropics "diffuses" into the extratropics due to atmospheric heat exchange, leading to a spillover of overcompensation into the extratropics.

4. Discussion

a. BJC in the MEMB

Taking into the full moisture effect in the MEMB (2.1), the MSE coefficient $M(x)$ introduces another spatial variation factor in the model. This spatial variation effect, however, can be absorbed largely into the feedback $b(x)$ in an equivalent dry EBM. Indeed, in the nondimensional MSE $E = M(x)T$, the MEMB (2.1) can be rewritten as

$$\partial_{xx}E - b_M(x)E + f(x) = 0, \tag{4.1}$$

where

$$b_M = \frac{b(x)}{M(x)} \tag{4.2}$$

will be called the MSE feedback parameter, to be distinguished from the temperature feedback parameter b. The MSE in (4.1) is determined by the same equation as temperature in the dry model [$M = 1$ in (2.1)], except for replacing $b(x)$ by $b_M(x)$. In the meantime, the local radiative equilibrium solution is

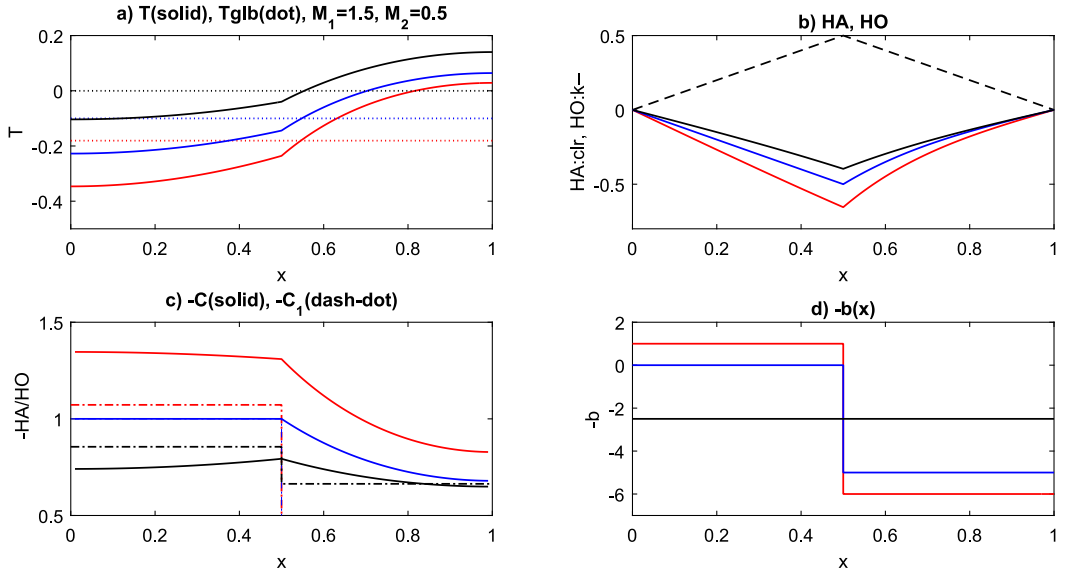

FIG. 6. Climate response of the two-zone solution (with $X = 0.5$) the same as in the dry model in Fig. 5, but in the MEMB with $M_1 = 1.5$ and $M_2 = 0.5$.

determined by $-b_M(x)E + f(x) = 0$ and therefore gives the same temperature response f/b as the dry model. Therefore, as $M(x)$ decreases poleward monotonically [from ~1.6 at the equator to ~0.4 at the pole; see discussion after Eq. (2.2b)], the moisture transport increases the amplitude of the temperature response poleward following $T = E/M$, with a ''polar amplification'' or ''tropical suppression.'' In addition, since the spatial scale of temperature change in the MEMB is determined by the MSE feedback as $1/b_M \sim M$ [see (4.1) and (D.1)], the decreasing M also reduces the spatial scale of the temperature response poleward, that is, the temperature gradient responds with a ''polar steepening'' or ''tropical flattening.''

The polar amplification and polar steepening can be seen in the solution in the two-zone MEMB, which assumes piecewise constant for $f(x)$ and $b(x)$ as in (3.1) and (3.2), as well as for $M(x)$ as

$$M(x) = \begin{cases} M_1 & 0 < x < X \\ M_2 & X < x < 1 \end{cases}. \tag{4.3}$$

The analytical solution can be derived similarly to the dry EBM (see appendix D). Figure 6 shows three solutions with a realistic magnitude of $M(x)$ variation: $M_1 = 1.5$ and $M_2 = 0.5$, while the feedback $b(x)$ remains the same as in the dry model in Fig. 5. Compared with the dry EBM (Fig. 5a), the polar warming is now enhanced in all the three cases (Fig. 6a). Physically, this polar amplification is caused by the poleward moisture transport (Cai 2005; Herweijer et al. 2005; Rose and Ferreira 2013), instead of a larger local positive feedback. Indeed, the polar amplification is generated even in the case of a uniform feedback $b_1 = b_2 = 2.5$ (black) from $T(1) \sim 0.1$ (Fig. 5a) to ~0.15 (Fig. 6a). Our study here gives an interpretation of this polar amplification from the MSE feedback perspective: the polar amplification can also be understood as a modification of the MSE feedback and the poleward steepening associated with the poleward moisture transport. The MSE now modifies the negative feedback from 2.5 to $b_{M2}(=2.5/0.5=5)$ in the extratropics and to $b_{M1}(=2.5/1.5=1.67)$ in the tropics [see Eq. (D.1)]. (It is interesting to note that, in spite of the polar warming amplification, there is a global mean cooling when $b_1 < b_2$, a point to be returned later.) In spite of these changes, the overall feature of the temperature response in the MEMB is similar to the dry EMB. As a result, the AHT and BJC ratio remain similar in both models (Figs. 6b,c vs Figs. 5b,c). Indeed, as seen in Fig. 7, the BJC ratio in the MEMB differs from that in the EMB by less than ~10% for a realistic range of moisture transport profiles.

b. BJC in CGCMs

Our theory can shed light on some important features of the previous BJC studies in complex GCMs, especially those in response to a perturbation OHT that has a zero global mean convergence, which is generated either directly by imposing an OHT in a coupled AGCM–slab ocean model (e.g., Broccoli et al. 2006; Kang et al. 2008, 2009; Seo et al. 2014), or indirectly by altering the Atlantic meridional overturning circulation (AMOC) in a CGCM (Zhang and Delworth 2005; Cheng et al. 2007;

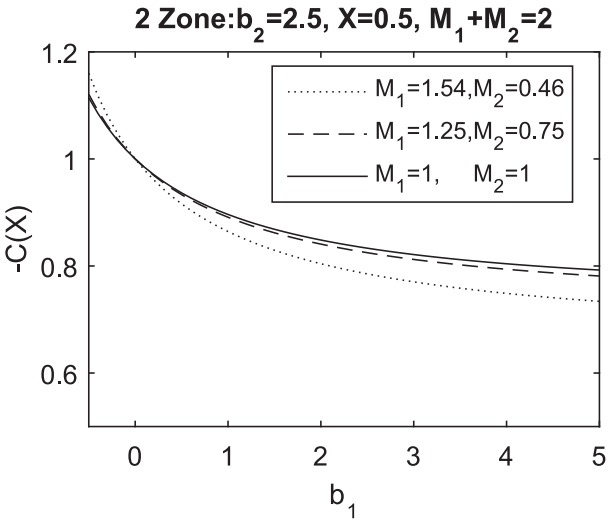

FIG. 7. The BJC ratio at the interzone boundary $x = X\ (=0.5)$ in the two-zone solution as a function of b_1 for three MSE coefficient profiles, $M_1 = 1$, $M_2 = 1$ (dry model); $M_1 = 1.25$, $M_2 = 0.75$; and $M_1 = 1.54$, $M_2 = 0.46$, with a fixed $b_2 = 2.5$.

Vellinga and Wu 2008; Zhang et al. 2010; Farneti and Vallis 2013; Yang et al. 2013). In a preliminary study, we have successfully applied our theory in the two-box version to a CGCM simulation of the climate evolution of the last 22 000 years (Yang et al. 2015b). A comprehensive and quantitative study that uses our EBM to diagnose the BJC in a CGCM is beyond the scope of this study. Instead, we will limit our application to some qualitative aspects in previous CGCM studies. This compromise is due partly to the uncertainties in a CGCM in the estimation of the spatial variation of climate feedback B (Feldl and Roe 2013b), and, moreover, the spatial variation of transport coefficient D or even the form of the AHT parameterization (Stone 1972, 1978b; Held 1999), especially in the tropics (Lindzen and Farrell 1980).

Qualitatively, in all these studies, the anomalous AHT has been found to transport in the opposite direction to the perturbation OHT. The fact that the AHT always compensates OHT across all these cases can be interpreted as the result of an overall stable climate in those models, which has to be dominated by a net negative climate feedback, presumably associated with the negative temperature feedback (Stone 1978a; Zhang et al. 1994; Soden et al. 2004; Soden and Held 2006). The dominant negative feedback in CGCMs may also explain that, in many cases and across most latitudes, the compensating AHT is weaker than the OHT, or undercompensation. In many CGCM studies forced by an OHT, the BJC ratio seems to be around 70%–80% (albeit with a large spread) in the extratropics (e.g., Zhang and Delworth 2005; van der Swaluw et al. 2007; Vellinga and Wu 2008; Zhang et al. 2010; Yang et al. 2013). This seems to be consistent with our theoretical estimation at the typical values of $b \sim 2$ to 3 (e.g., Fig. 1).

In particular, a robust feature in many models is a compensating AHT that exceeds the magnitude of the OHT in certain latitude ranges, especially in the tropics (e.g., Fig. 4 of Vellinga and Wu 2008; Fig. 5 of Zhang et al. 2010; Figs. 6 and 12 of Kang et al. 2008; Fig. 15 of Kang et al. 2009; Fig. 2 of Yang et al. 2013; Fig. 6 of Rose and Ferreira 2013; Fig. 3 of Seo et al. 2014). Idealized model experiments and feedback analyses have shown substantial sensitivity of the BJC to climate feedbacks, such as cloud feedback (e.g., Kang et al. 2008, 2009; Zhang et al. 2010; Zelinka and Hartmann 2012; Seo et al. 2014; Huang and Zhang 2014) and ice–albedo feedback (e.g., North 1975; Wang and Stone 1980; Enderton and Marshall 2009). Some GCM studies have been diagnosed and interpreted using an EBM. The interpretation has focused on the global features instead of the regional BJC, in particular, the regional overcompensation. Indeed, all of these EBMs have adopted a uniform negative climate feedback ($b > 0$ in our notation here), none of which is able to reproduce the overcompensation in their GCM experiments (e.g., Fig. 15 of Kang et al. 2009; Fig. 14 of Farneti and Vallis 2013; Fig. 3 of Seo et al. 2014). Rose and Ferreira's (2013) study is an exception, where a two-box model with a uniform feedback generates an overcompensation by representing the additional positive feedback as a reduction of the local forcing, as noted earlier. Here, our study suggests that the overcompensation in the tropics in these models can be understood more naturally from the unified BJC perspective as the result of a local positive feedback. Many recent modeling studies suggest that climate feedback is dominated by a net positive feedback in the tropics, associated with the water vapor feedback and cloud feedback (Zhang et al. 1994; Zelinka and Hartmann 2012; Feldl and Roe 2013a; Roe et al. 2015). The positive cloud feedback can be caused by either an increased deep convection and the subsequent positive feedback on longwave cloud forcing (Kang et al. 2008; Hwang and Frierson 2010) or the positive feedback between low stratus cloud and SST and the associated shortwave cloud forcing (Philander et al. 1996; Clement et al. 2009). When the cloud is prescribed in the GCMs, the BJC ratio is greatly reduced, mostly being undercompensation (e.g., Kang et al. 2008, 2009; Zhang et al. 2010; Seo et al. 2014). Thus, an active cloud feedback seems to be crucial for generating overcompensation in many GCMs.

c. Global mean temperature

It has been seen in Figs. 3a, 5a, and 6a that, given an OHT forcing, the spatial variation of feedback will change not only the temperature gradient, AHT and BJC, but also the global mean temperature. Indeed, from Eq. (3.3), or more generally Eq. (D.1), the global mean temperature can be derived as

$$\overline{T} = (1 + C_X)\left(\frac{1}{b_2} - \frac{1}{b_1}\right)H_{OX}. \tag{4.4}$$

As long as the feedback is uniform $b_1 = b_2$, $\overline{T} = 0$, as seen in Figs. 3a, 5a, and 6a (black). If $b_2 > b_1$, however, note that a negative feedback $b_1 > 0$ leads to undercompensation and a weakly positive feedback $b_1 < 0$ leads to overcompensation; Eq. (4.4) shows that a northward OHT generates a global cooling $\overline{T} < 0$, as in Figs. 3a, 5a, and 6a (blue and red). This effect of nonuniform feedback on global mean temperature can be shown valid in the full MEMB (2.1). With the no-flux boundary condition, a global average of (2.1) yields (Armour et al. 2013)

$$\overline{T} = -\overline{b'T'}/\overline{b} + \overline{f}/\overline{b}, \tag{4.5}$$

where the temperature and feedback have been decomposed as the global mean (overbar) and deviation (prime). For OHT forcing of $\overline{f(x)} = 0$, $\overline{T} = 0$ if the feedback is uniform, $b(x)' = 0$. Otherwise, a global mean temperature response is induced by the spatial covariance between feedback a global mean temperature and it contributes significantly to the global climate sensitivity (Armour et al. 2013; Roe et al. 2015). A positive correlation between the (negative) feedback strength and temperature leads to a global cooling and vice versa. Since a northward OHT always increases the temperature poleward, an enhanced (negative) feedback poleward will lead to a global cooling, consistent with the two-zone solution in (4.4). Furthermore, (4.5) shows that the global cooling intensifies if the global feedback strength $\overline{b}$ weakens, consistent with the intensified global cooling when tropical feedback becomes positive (Figs. 3a, 5a, and 6a). Physically, this global cooling is caused by a greater negative feedback in the extratropics, which damps the local warming more than the damping of cooling in the tropics, and will then lead to a global mean cooling. This is the ''radiator fin'' mechanism proposed by Pierrehumbert (1995). On the other hand, if the extratropical climate feedback is enhanced by additional positive feedbacks, such as water vapor feedback and high-latitude convective cloud feedback, such that $b_2 < b_1$ in (4.4), a northward OHT will lead to a warming in the global mean. The extratropical warming also enhances the anomalous poleward temperature gradient, with a polar amplification. This polar amplification reduces the climatological pole-to-equator temperature gradient, providing a potential mechanism for a warmer climate with reduced temperature gradient, or the so-called equable climate (Abbot and Tziperman 2008; Rose and Ferreira 2013).

d. Response to general climate forcing

We have so far confined our study to the response of the AHT to a perturbation OHT forcing. For a general perturbation climate forcing, such as that for a global warming, it can always be decomposed into two parts: the global mean that is spatially uniform $\overline{f}$ and a residual that has a zero global mean f'. The residual forcing f' can always be combined with the true OHT and decomposed to the convergence of an "equivalent OHT" as in Eq. (2.4). Our BJC study above still applies if we define the BJC as the ratio between the responses of the AHT and the equivalent OHT.

In contrast, in response to the global mean forcing $\overline{f}$, our BJC result may not apply. First of all, $\overline{f}$ cannot be decomposed into the convergence of an equivalent OHT as in Eq. (2.4). Yet, it can still induce a response in the AHT if the feedback is spatially nonuniform. For example, in our two-zone solution (3.3) to (3.5), a temperature gradient is generated by the gradient of the radiative equilibrium temperature $T_{f2} - T_{f1} = f_2/b_2 - f_1/b_1$. For a uniform heating $f_2 = f_1 = f > 0$, if, for example, $b_1 < b_2$, we will have

$$T_{f2} - T_{f1} = \frac{f_2}{b_2} - \frac{f_1}{b_1} = f\left(\frac{1}{b_2} - \frac{1}{b_1}\right) < 0. \tag{4.6}$$

This will lead to $G < 0$ in (3.5), an equatorward increase of temperature and then a poleward AHT $H_A(x) > 0$. Now, the uniform forcing heats the tropics more than the extratropics because of the weaker negative feedback in the tropics. This tropical warming response appears similar to that in response to an equatorward OHT. However, one cannot derive the BJC ratio explicitly unless the OHT response is also parameterized and in turn calculated explicitly. Now, there is no guarantee that the AHT is even of the opposite sign to the OHT, as will be shown in an accompanying study in a coupled box model (Yang et al. 2015a). As an extreme example here, if the OHT can be parameterized as $H_o = -p\partial_x T$, as the AHT (Farneti and Vallis 2013), the BJC ratio will remain positive, $C = H_A/H_o = 1/p > 0$, and there is no longer compensation between AHT and OHT. This is similar to the response in the coupled system of the atmosphere and oceanic wind-driven gyre (Held 2001; Farneti and Vallis 2013). This uncertainty of the BJC to a general climate forcing is also another cause of the diverse BJC ratio in previous studied, some

of which are perturbed by an OHT and others by global warming forcing.

It is worth noting that although our model cannot determine the response of the BJC to a general climate forcing, on account of the lack of the OHT parameterization, our theory can be extended directly to studying the response of the total PHT to a general climate forcing (Stone 1978a) as long as the PHT can be parameterized proportional to the temperature gradient. Under a uniform global warming forcing discussed above, the additional positive feedback associated with water vapor feedback and cloud feedback reduces the negative tropical feedback or even reverses it to local positive feedback. As discussed in (4.6), this should generate a poleward PHT, consistent with the analyses of multiple CGCM simulations by Zelinka and Hartmann (2012).

5. Conclusions

A theory is developed in an EBM to understand the response of the AHT to perturbation OHT forcing, with the focus on the role of the climate feedback, and particularly its spatial variation. In general, for a stable climate dominated by negative climate feedback, the AHT always compensates the OHT; that is, the BJC is always valid. More quantitatively, if the feedback is negative everywhere, the compensating AHT is weaker than the OHT, or an undercompensation, because of the surface heating is partly damped through the TOA loss of energy, leaving less energy to be transport back by the AHT. The BJC ratio increases when the negative feedback strength decreases or the heat transport efficiency increases. One novel finding in our 1D EMB is that the BJC ratio depends on the spatial scale of the forcing, and tends to be bounded between a minimum of undercompensation at the planetary scale and the maximum of perfect compensation at small scales, as long as the climate feedback remains largely negative. Most interestingly, our theory suggests that the BJC ratio can be changed significantly by the spatial variation of climate feedback. In particularly, the BJC ratio is enhanced significantly by a local positive feedback such that an overcompensation can be generated by a regional positive feedback, because the positive feedback increases the local temperature response, the anomalous temperature gradient, and in turn the compensating AHT. Finally, the inclusion of the poleward latent heat transport does not change the BJC significantly, although it does lead to a significant polar amplification accompanied by a polar steepening of the temperature gradient. Our theory sheds some lights on previous studies in complex GCMs. In particular, our theory suggests that the overcompensation in these models is contributed by the positive feedback in the tropics.

Further work is needed to understand the BJC in complex GCMs and, eventually, the real world. Our BJC study is subject to two major assumptions in the EBM: the linear parameterization of the AHT to temperature gradient and the linear climate feedback parameterization in terms of the local temperature. Our preliminary test shows that the major conclusions here are not sensitive to the linear AHT parameterization. We have repeated the BJC study here using two nonlinear parameterization schemes with the transport coefficient proportional to 0.5 and first power of the temperature gradient [i.e., $H_A \sim -\partial_x(|T|^{1/2}T)$ and $H_A \sim -\partial_x(|T|T)$], as implied by some previous studies (Stone 1972, 1978b; Held 1999). As in the linear scheme, the BJC still exhibits undercompensation when the feedback remains negative across the latitude, while the overcompensation is generated when the local feedback becomes positive (not shown). Indeed, regardless of the AHT parameterization, physically the BJC should remain in undercompensation if the feedback is negative everywhere, because the negative feedback damps the local heating effect and in turn the temperature response. When the local feedback vanishes (e.g., in the tropics $b_1 = 0$), the EBM (2.1) can be shown to generate a perfect compensation $C = -1$ in the tropics as long as the AHT satisfies the no flux condition at the equator. Therefore, an overcompensation should be generated if the local feedback crosses this zero feedback to become positive.

The parameterization of local feedback, however, remains as a complex issue. In more complex models and the real world, local climate feedback could change with the dynamics itself, such as the moisture transport and water vapor feedback (Cai 2005; Herweijer et al. 2005) and cloud feedback (Abbot and Tziperman 2008). As such, climate feedback may not even be constant linear functions of local surface temperature as is commonly assumed in feedback analysis, particularly when forced by OHT (Rose and Ferreira 2013; Rose et al. 2014). In addition, an accurate estimation of regional climate feedback remains challenging, even in a GCM. An accurate estimation of each feedback in a GCM requires offline calculations using, for example, the kernel method (e.g., Soden et al. 2004). Even more challenging is the estimation of the spatial structure of the feedback, which could differ for different definitions because of the interaction of climate responses in different regions through the energy transport (Feldl and Roe 2013b; Rose et al. 2014; Roe et al. 2015). Finally, as

discussed earlier, the estimation of the spatial pattern of the relative feedback b [Eq. (2.3)] depends not only on the feedback B itself, but also on the heat transport coefficient D, whose spatial structure remain highly uncertain (e.g., Stone 1972, 1978b; Lindzen and Farrell 1980; Held 1999). A careful study is needed to determine how well our theory can be used to diagnose the BJC in a CGCM quantitatively. The assessment of the BJC in the real world is even more challenging because of the difficulty to estimate feedback and transport efficiency from the observations available. Indeed, for the real world, even the estimation of the global climate feedback and sensitivity remains highly uncertain (Lindzen and Choi 2011). Therefore, much further work is needed to understand the potential effect of the climate feedback.

Acknowledgments. We thank three reviewers for their helpful comments. This work is supported by Chinese MOST 2012CB955201 and NSFC (41130105, 41376007, 41176002), US NSF, and DOE.

APPENDIX A

BJC on a Sphere for Uniform Feedback

The nondimensional form of EBM on the sphere can be written as (North 1975)

$$\frac{\partial}{\partial x}\left[(1-x^2)\frac{\partial}{\partial x}(MT)\right]-b(x)T+f(x)=0, \quad \text{for} \quad 0<x<1. \tag{A.1}$$

The AHT is parameterized as

$$H_A=-(1-x^2)^{1/2}\frac{\partial(MT)}{\partial x}. \tag{A.2}$$

The oceanic heat balance is

$$f(x)=-\frac{\partial}{\partial x}[(1-x^2)^{1/2}H_O]. \tag{A.3}$$

A single hemisphere solution has the no-flux $H_A=0$ boundary condition at $x=0$, 1. For a uniform feedback b and a constant M, the response can be derived analytically in terms of the even-order Legendre polynomials $P_m(x)$, $m=2, 4, \ldots$ (North 1975):

$$P_0(x)=1, \quad P_2(x)=\frac{3x^2-1}{2}, \ldots . \tag{A.4}$$

For a surface forcing of the form of a Legendre polynomial, $f(x)=f_mP_m(x)$, the corresponding OHT can be obtained from the ocean budget (A.3) as

$$H_O=\frac{f_m}{m(m+1)}(1-x^2)^{1/2}\frac{\partial P_m}{\partial x} \tag{A.5}$$

after using the identity

$$-\frac{d}{dx}\left[(1-x^2)\frac{d}{dx}P_m\right]=m(m+1)P_m. \tag{A.6}$$

Similarly, the temperature response can be derived from (A.1) as

$$T(x)=T_mP_m(x), \quad \text{where} \quad T_m=\frac{f_m}{m(m+1)+b}. \tag{A.7}$$

The BJC ratio is therefore

$$C_m^S=\frac{H_A}{H_O}=\frac{-1}{1+b/[m(m+1)]}<0. \tag{A.8}$$

APPENDIX B

Stability of the Two-Zone System

The eigenvalue equation for the plane system can be derived by substituting $T\sim e^{\lambda t}$ into the atmospheric Eq. (2.1) and the time-dependent slab oceanic heat budget (2.9) as

$$\partial_{xx}[M(x)T]-[b(x)+\lambda]T=0. \tag{B.1}$$

With the no-flux boundary conditions (2.12), we have an integral constrain on the eigenvalue as

$$\lambda\int_0^1(MT)^2\,dx=-\left\{\int_0^1\left[\frac{d(MT)}{dx}\right]^2dx+\int_0^1b(x)MT^2\,dx\right\}. \tag{B.2}$$

Since $M>0$, the eigenvalue will be negative and the system is stable if the feedback is nonpositive, $-b(x)\le 0$.

For the two-zone feedback in Eq. (3.1), the eigenvalue equation can be derived as

$$\sqrt{\lambda+b_2}\tanh[\sqrt{\lambda+b_2}(X-1)]=\sqrt{\lambda+b_1}\tanh(\sqrt{\lambda+b_1}X). \tag{B.3}$$

In the limit of weak feedback, b_1, $b_2\to 0$, the eigenvalue approaches the global mean feedback

$$\lambda \to -[b_1 X + b_2(1-X)] = \overline{b}. \tag{B.4}$$

For general b_1, and b_2, numerical solutions of (B.3) found that the eigenvalue of the least damped mode can still be approximated well by (B.4), although (B.4) is usually slightly more positive than the true eigenvalue from (B.3) (see examples in Fig. 4b).

APPENDIX C

BJC in a Two-Box Model

All the conclusions on BJC in our two-zone model can also be obtained in a two-box model, which has been used previously for the study of climate sensitivity and climate stability (Marotzke and Stone 1995; Bates 2012). In nondimensional variables, the TOA radiative flux for box i is parameterized as $F_i = a_i - b_i T_i$, $i = 1, 2$, and the poleward AHT as $H_A = T_2 - T_1$. The response to a perturbation OHT H_O is determined by the energy balance in the coupled atmosphere–slab ocean model as

$$0 = -b_1 T_1 + (T_2 - T_1) + H_O, \tag{C.1a}$$
$$0 = -b_2 T_2 - (T_2 - T_1) - H_O. \tag{C.1b}$$

The BJC ratio can be derived as

$$C^B \equiv \frac{-1}{1 + b_1 b_2/(b_1 + b_2)}. \tag{C.2}$$

The stability condition can be derived by solving the eigenvalue problem in the presence of heat storage in Eqs. (C.1a) and (C.1b) as $b_1 b_2 + (b_1 + b_2) \ge 0$. Therefore, the climate system is stable (unstable) if feedbacks are all negative (positive). In the case of a local positive feedback, say, $-b_1 > 0$, the coupled system is still stable as long as the positive feedback is not too strong, $0 < -b_1 < b_2/(b_2 + 1)$. Thus, $C^B < 0$ always holds for a stable climate, and the compensation is enhanced from undercompensation for negative feedback to overcompensation for a regional positive feedback.

APPENDIX D

BJC in Two-Zone MEMB

Using Eq. (2.1) or (4.1), and the matching boundary condition of the continuity of temperature and heat flux across the interzone boundary, we have the temperature response to the surface forcing (3.7) as

$$T(x) = \begin{cases} \dfrac{G}{M_1\sqrt{b_{M1}}}\dfrac{\cosh(\sqrt{b_{M1}}x)}{\sinh(\sqrt{b_{M1}}X)} + T_{f1}, & 0 \le x \le X, \\ \dfrac{G}{M_2\sqrt{b_{M2}}}\dfrac{\cosh[\sqrt{b_{M2}}(x-1)]}{\sinh[\sqrt{b_{M2}}(X-1)]} + T_{f2}, & X \le x \le 1, \end{cases} \tag{D.1}$$

where

$$G = \frac{\Delta F\left[\dfrac{1}{b_1 X} + \dfrac{1}{b_2(1-X)}\right]}{\dfrac{\coth(\sqrt{b_{M1}}X)}{M_1\sqrt{b_{M1}}} + \dfrac{\coth[\sqrt{b_{M2}}(1-X)]}{M_2\sqrt{b_{M2}}}}. \tag{D.2}$$

The corresponding AHT is

$$H_A(x) = \begin{cases} H_{AX}\dfrac{\sinh(\sqrt{b_{M1}}x)}{\sinh(\sqrt{b_{M1}}X)}, & 0 \le x \le X, \\ H_{AX}\dfrac{\sinh[\sqrt{b_{M2}}(x-1)]}{\sinh[\sqrt{b_{M2}}(X-1)]}, & X < x \le 1, \end{cases} \tag{D.3}$$

with $H_{AX} \equiv H_A(X) = -G$. With the $H_{OX} \equiv H_O(X) = -\Delta F$, the BJC ratio is

$$C(x) = \begin{cases} C_X\dfrac{\sinh(\sqrt{b_{M1}}x)}{\sinh(\sqrt{b_{M1}}X)}\dfrac{X}{x}, & 0 \le x \le X, \\ C_X\dfrac{\sinh[\sqrt{b_{M2}}(x-1)]}{\sinh[\sqrt{b_{M2}}(X-1)]}\dfrac{X-1}{x-1}, & X < x \le 1, \end{cases} \tag{D.4a}$$

with the BJC ratio at the interzone boundary as

$$C_X = C(X) = \frac{H_{AX}}{H_{OX}} = \frac{-\left[\dfrac{1}{b_1 X} + \dfrac{1}{b_2(1-X)}\right]}{\dfrac{\coth(\sqrt{b_{M1}}X)}{M_1\sqrt{b_{M1}}} + \dfrac{\coth[\sqrt{b_{M2}}(1-X)]}{M_2\sqrt{b_{M2}}}}. \tag{D.4b}$$

REFERENCES

Abbot, D. S., and E. Tziperman, 2008: A high-latitude convective cloud feedback and equable climates. *Quart. J. Roy. Meteor. Soc.*, **134**, 165–185, doi:10.1002/qj.211.

Armour, K., C. M. Bitz, and G. H. Roe, 2013: Time-varying climate sensitivity from regional feedbacks. *J. Climate*, **26**, 4518–4534, doi:10.1175/JCLI-D-12-00544.1.

Bates, J. R., 2012: Climate stability and sensitivity in some simple conceptual models. *Climate Dyn.*, **38**, 455–473, doi:10.1007/s00382-010-0966-0.

Bender, C. M., and S. A. Orszag, 1978: *Advanced Mathematical Methods for Scientists and Engineers I: Asymptotic Methods and Perturbation Theory*. McGraw Hill, 593 pp.

Bjerknes, J., 1964: Atlantic air/sea interaction. *Advances in Geophysics*, Vol. 10, Academic Press, 1–82.

Broccoli, A. J., K. A. Dahl, and R. J. Stouffer, 2006: Response of the ITCZ to Northern Hemisphere cooling. *Geophys. Res. Lett.*, **33**, L01702, doi:10.1029/2005GL024546.

Budyko, M. I., 1969: The effect of solar radiation variations on the climate of the earth. *Tellus*, **21A**, 611–619, doi:10.1111/j.2153-3490.1969.tb00466.x.

Cai, M., 2005: Dynamical amplification of polar warming. *Geophys. Res. Lett.*, **32**, L22710, doi:10.1029/2005GL024481.

Cheng, W., C. M. Bitz, and J. C. H. Chiang, 2007: Adjustment of the global climate to an abrupt slowdown of the Atlantic meridional overturning circulation. *Ocean Circulation: Mechanisms and Impacts*, *Geophys. Monogr.*, Vol. 173, 295–313, doi:10.1029/173GM19.

Clement, A. C., and R. Seager, 1999: Climate and the tropical oceans. *J. Climate*, **12**, 3383–3401, doi:10.1175/1520-0442(1999)012<3383:CATTO>2.0.CO;2.

——, R. Burgman, and J. R. Norris, 2009: Observational and model evidence for positive low-level cloud feedback. *Science*, **325**, 460–464, doi:10.1126/science.1171255.

Donohoe, A., J. Marshall, D. Ferreira, and D. Mcgee, 2013: The relationship between ITCZ location and cross-equatorial atmospheric heat transport: From the seasonal cycle to the Last Glacial Maximum. *J. Climate*, **26**, 3597–3618, doi:10.1175/JCLI-D-12-00467.1.

Enderton, D., and J. Marshall, 2009: Explorations of atmosphere–ocean–ice climates on an aquaplanet and their meridional energy transports. *J. Atmos. Sci.*, **66**, 1593–1611, doi:10.1175/2008JAS2680.1.

Farneti, R., and G. Vallis, 2013: Meridional energy transport in the coupled atmosphere–ocean system: Compensation and partitioning. *J. Climate*, **26**, 7151–7166, doi:10.1175/JCLI-D-12-00133.1.

Feldl, N., and G. H. Roe, 2013a: The nonlinear and nonlocal nature of climate feedbacks. *J. Climate*, **26**, 8289–8304, doi:10.1175/JCLI-D-12-00631.1.

——, and ——, 2013b: Four perspectives on climate feedbacks. *Geophys. Res. Lett.*, **40**, 4007–4011, doi:10.1002/grl.50711.

Frierson, D. M. W., and Y.-T. Hwang, 2012: Extratropical influence on ITCZ shifts in slab ocean simulations of global warming. *J. Climate*, **25**, 720–733, doi:10.1175/JCLI-D-11-00116.1.

——, I. Held, and P. Zurita-Gotor, 2007: A grey-radiation aquaplanet moist GCM. Part II: Energy transports in altered climates. *J. Atmos. Sci.*, **64**, 1680–1693, doi:10.1175/JAS3913.1.

Gregory, J., and J. Mitchell, 1997: The climate response to CO_2 of the Hadley Centre coupled AOGCM with and without flux adjustment. *Geophys. Res. Lett.*, **24**, 1943–1946, doi:10.1029/97GL01930.

Held, I., 1999: The macroturbulence of the troposphere. *Tellus*, **51A**, 59–70, doi:10.1034/j.1600-0870.1999.t01-1-00006.x.

——, 2001: The partitioning of the poleward energy transport between the tropical ocean and atmosphere. *J. Atmos. Sci.*, **58**, 943–948, doi:10.1175/1520-0469(2001)058<0943:TPOTPE>2.0.CO;2.

Herweijer, C., R. Seager, M. Winton, and A. Clement, 2005: Why ocean heat transport warms the global mean climate. *Tellus*, **57A**, 662–675, doi:10.1111/j.1600-0870.2005.00121.x.

Huang, Y., and M. Zhang, 2014: The implication of radiative forcing and feedback for meridional energy transport. *Geophys. Res. Lett.*, **41**, 1665–1672, doi:10.1002/2013GL059079.

Hwang, Y.-T., and D. M. Frierson, 2010: Increasing atmospheric poleward energy transport with global warming. *Geophys. Res. Lett.*, **37**, L24807, doi:10.1029/2010GL045440.

Kang, S. M., I. M. Held, D. M. W. Frierson, and M. Zhao, 2008: The response of the ITCZ to extratropical thermal forcing: Idealized slab-ocean experiments with a GCM. *J. Climate*, **21**, 3521–3532, doi:10.1175/2007JCLI2146.1.

——, D. M. W. Frierson, and I. M. Held, 2009: The tropical response to extratropical thermal forcing in an idealized GCM: The importance of radiative feedbacks and convective parameterization. *J. Atmos. Sci.*, **66**, 2812–2827, doi:10.1175/2009JAS2924.1.

Lindzen, R. S., and B. Farrell, 1980: The role of the polar regions in global climate, and a new parameterization of global heat transport. *Mon. Wea. Rev.*, **108**, 2064–2079, doi:10.1175/1520-0493(1980)108<2064:TROPRI>2.0.CO;2.

——, and Y.-S. Choi, 2011: On the observational determination of climate sensitivity and its implications. *Asia-Pac. J. Atmos. Sci.*, **47**, 377–390, doi:10.1007/s13143-011-0023-x.

Manabe, S., K. Bryan, and M. J. Spelman, 1975: A global ocean–atmosphere climate model. Part I: The atmospheric circulation. *J. Phys. Oceanogr.*, **5**, 3–29, doi:10.1175/1520-0485(1975)005<0003:AGOACM>2.0.CO;2.

Marotzke, J., and P. Stone, 1995: Atmospheric transports, the thermohaline circulation, and flux adjustments in a simple coupled model. *J. Phys. Oceanogr.*, **25**, 1350–1364, doi:10.1175/1520-0485(1995)025<1350:ATTTCA>2.0.CO;2.

North, G. R., 1975: Theory of energy-balance climate models. *J. Atmos. Sci.*, **32**, 2033–2043, doi:10.1175/1520-0469(1975)032<2033:TOEBCM>2.0.CO;2.

Philander, S. G. H., D. Gu, D. Halpern, G. Lambert, N.-C. Lau, T. Li, and R. C. Pacanowski, 1996: Why the ITCZ is mostly north of the equator. *J. Climate*, **9**, 2958–2972, doi:10.1175/1520-0442(1996)009<2958:WTIIMN>2.0.CO;2.

Pierrehumbert, R., 1995: Thermostats, radiator fins, and the local runaway greenhouse. *J. Atmos. Sci.*, **52**, 1784–1806, doi:10.1175/1520-0469(1995)052<1784:TRFATL>2.0.CO;2.

Rahmstorf, S., 1996: On the freshwater forcing and transport of the Atlantic thermohaline circulation. *Climate Dyn.*, **12**, 799–811, doi:10.1007/s003820050144.

Roe, G. H., N. Feldl, K. C. Armour, Y.-T. Hwang, and D. M. Frierson, 2015: The remote impacts of climate feedbacks on regional climate predictability. *Nat. Geosci.*, **8**, 135–139, doi:10.1038/ngeo2346.

Rose, B. E., and D. Ferreira, 2013: Ocean heat transport and water vapor greenhouse in a warm equable climate: A new look at the low gradient paradox. *J. Climate*, **26**, 2117–2136, doi:10.1175/JCLI-D-11-00547.1.

——, K. C. Armour, D. S. Battisti, N. Feldl, and D. D. Koll, 2014: The dependence of transient climate sensitivity and radiative feedbacks on the spatial pattern of ocean heat uptake. *Geophys. Res. Lett.*, **41**, 1071–1078, doi:10.1002/2013GL058955.

Sellers, W. D., 1969: A global climate model based on the energy balance of the Earth–atmosphere system. *J. Appl. Meteor.*, **8**, 392–400, doi:10.1175/1520-0450(1969)008<0392:AGCMBO>2.0.CO;2.

Seo, J., S. M. Kang, and D. M. Frierson, 2014: Sensitivity of intertropical convergence zone movement to the latitudinal position of thermal forcing. *J. Climate*, **27**, 3035–3042, doi:10.1175/JCLI-D-13-00691.1.

Shaffrey, L., and R. Sutton, 2006: Bjerknes compensation and the decadal variability of the energy transports in a coupled climate model. *J. Climate*, **19**, 1167–1181, doi:10.1175/JCLI3652.1.

Soden, B. J., and I. Held, 2006: An assessment of climate feedbacks in coupled ocean–atmosphere models. *J. Climate*, **19**, 3354–3360, doi:10.1175/JCLI3799.1.

——, A. J. Broccoli, and R. S. Hemler, 2004: On the use of cloud forcing to estimate cloud feedback. *J. Climate*, **17**, 3661–3665, doi:10.1175/1520-0442(2004)017<3661:OTUOCF>2.0.CO;2.

Stommel, H., 1961: Thermohaline convection with two stable regimes of flow. *Tellus*, **13A**, 224–230, doi:10.1111/j.2153-3490.1961.tb00079.x.

Stone, P. H., 1972: A simplified radiative-dynamical model for the static stability of rotating atmospheres. *J. Atmos. Sci.*, **29**, 405–418, doi:10.1175/1520-0469(1972)029<0405:ASRDMF>2.0.CO;2.

——, 1978a: Constraints on dynamical transports of energy on a spherical planet. *Dyn. Atmos. Oceans*, **2**, 123–139, doi:10.1016/0377-0265(78)90006-4.

——, 1978b: Baroclinic adjustment. *J. Atmos. Sci.*, **35**, 561–571, doi:10.1175/1520-0469(1978)035<0561:BA>2.0.CO;2.

Taylor, P. C., R. G. Ellingson, and M. Cai, 2011: Geographic distribution of climate feedbacks in the NCAR CCSM3.0. *J. Climate*, **24**, 2737–2753, doi:10.1175/2010JCLI3788.1.

Trenberth, K., and J. M. Caron, 2001: Estimates of meridional atmosphere and ocean heat transports. *J. Climate*, **14**, 3433–3443, doi:10.1175/1520-0442(2001)014<3433:EOMAAO>2.0.CO;2.

Vallis, G. K., and R. Farneti, 2009: Meridional energy transport in the coupled atmosphere–ocean system: Scaling and numerical experiments. *Quart. J. Roy. Meteor. Soc.*, **135**, 1643–1660, doi:10.1002/qj.498.

van der Swaluw, E., S. S. Drijfhout, and W. Hazeleger, 2007: Bjerknes compensation at high northern latitudes: The ocean forcing the atmosphere. *J. Climate*, **20**, 6023–6032, doi:10.1175/2007JCLI1562.1.

Vellinga, M., and P. Wu, 2008: Relationship between northward ocean and atmosphere energy transports in a coupled climate model. *J. Climate*, **21**, 561–575, doi:10.1175/2007JCLI1754.1.

Wang, W.-C., and P. Stone, 1980: Effect of ice–albedo feedback on global sensitivity in a one-dimensional radiative-convective climate model. *J. Atmos. Sci.*, **37**, 545–552, doi:10.1175/1520-0469(1980)037<0545:EOIAFO>2.0.CO;2.

Winton, M., 2003: On the climatic impact of ocean circulation. *J. Climate*, **16**, 2875–2889, doi:10.1175/1520-0442(2003)016<2875:OTCIOO>2.0.CO;2.

Wunsch, C., 2005: The total meridional heat flux and its oceanic and atmospheric partition. *J. Climate*, **18**, 4374–4380, doi:10.1175/JCLI3539.1.

Yang, H., and H. Dai, 2015: Effect of wind forcing on the meridional heat transport in a coupled climate model: Equilibrium response. *Climate Dyn.*, **45**, 1451–1470, doi:10.1007/s00382-014-2393-0.

——, Y. Wang, and Z. Liu, 2013: A modelling study of the Bjerknes compensation in the meridional heat transport in a freshening ocean. *Tellus*, **65A**, 18480, doi:10.3402/tellusa.v65i0.18480.

——, Y. Zhao, and Z. Liu, 2015a: Understanding Bjerknes compensation in atmosphere and ocean heat transports using a coupled box model. *J. Climate*, doi:10.1175/JCLI-D-15-0281.1, in press.

——, ——, ——, Q. Li, F. He, and Q. Zhang, 2015b: Heat transport compensation in atmosphere and ocean over the past 22,000 years. *Sci. Rep.*, **5**, 16661, doi:10.1038/srep16661.

Zelinka, M. D., and D. L. Hartmann, 2012: Climate feedbacks and their implications for poleward energy flux changes in a warming climate. *J. Climate*, **25**, 608–624, doi:10.1175/JCLI-D-11-00096.1.

Zhang, M., J. Hack, J. Kiehl, and R. Cess, 1994: Diagnostic study of climate feedback processes in atmospheric general circulation models. *J. Geophys. Res.*, **99**, 5525–5537, doi:10.1029/93JD03523.

Zhang, R., and T. Delworth, 2005: Simulated tropical response to a substantial weakening of the Atlantic thermohaline circulation. *J. Climate*, **18**, 1853–1860, doi:10.1175/JCLI3460.1.

——, S. M. Kang, and I. M. Held, 2010: Sensitivity of climate change induced by weakening of the Atlantic meridional overturning circulation to cloud feedback. *J. Climate*, **23**, 378–389, doi:10.1175/2009JCLI3118.1.